

## Article

# Effect of Variable-Nozzle-Turbocharger-Coupled Exhaust Gas Recirculation on Natural Gas Engine Emissions and Collaborative Optimization

Kan Zhu <sup>1</sup>, Diming Lou <sup>1</sup>, Yunhua Zhang <sup>1,\*</sup> , Yedi Ren <sup>1</sup>  and Lanlan Fan <sup>2</sup>

<sup>1</sup> School of Automotive Studies, Tongji University, Shanghai 201804, China; zhuk\_74@tongji.edu.cn (K.Z.); loudiming@tongji.edu.cn (D.L.); renyedi1993@163.com (Y.R.)

<sup>2</sup> Jinan Power Co., Ltd., Sinotruk Group, Ji'nan 250101, China; fanlanlan@sinotruk.com

\* Correspondence: zhangyunhua313@163.com

**Abstract:** Equivalent combustion natural gas engines typically utilize exhaust gas recirculation (EGR) systems to tackle their high thermal burden and NO<sub>x</sub> emissions. Variable nozzle turbochargers (VNT) can increase the engine intake and EGR rate simultaneously, resulting in NO<sub>x</sub> reduction while ensuring robust power performance. Using a VNT along with engine bench testing, the impact of VNT- and EGR-coordinated control on the performance and emissions of equivalent combustion natural gas engines was investigated under different operating conditions. Subsequently, multi-objective optimization was performed using a support vector machine. The results demonstrated that the use of VNTs in equivalent combustion natural gas engines could bolster the capacity to introduce EGR under several operative conditions and extend the scope of EGR regulation, thereby decreasing the engine's thermal burden, improving fuel efficiency, and curbing emissions. Owing to the implementation of a multi-objective optimization method based on a support vector regression model and NSGA-II genetic algorithm, VNT and EGR control parameters could be optimized to slightly improve the economy and significantly reduce NO<sub>x</sub> emissions while maintaining the original engine power performance. At 20 operating points optimized for validation, brake-specific fuel consumption (BSFC) and NO<sub>x</sub> decreased by 0.94% and 47.0%, respectively, and CH<sub>4</sub> increased by 3.7%, on average.

**Keywords:** natural gas engine; EGR; emissions; support vector machine; optimization



**Citation:** Zhu, K.; Lou, D.; Zhang, Y.; Ren, Y.; Fan, L. Effect of Variable-Nozzle-Turbocharger-Coupled Exhaust Gas Recirculation on Natural Gas Engine Emissions and Collaborative Optimization. *Machines* **2024**, *12*, 260. <https://doi.org/10.3390/machines12040260>

Academic Editor: Davide Astolfi

Received: 2 March 2024

Revised: 7 April 2024

Accepted: 12 April 2024

Published: 15 April 2024



**Copyright:** © 2024 by the authors. Licensee MDPI, Basel, Switzerland. This article is an open access article distributed under the terms and conditions of the Creative Commons Attribution (CC BY) license (<https://creativecommons.org/licenses/by/4.0/>).

## 1. Introduction

In comparison to gasoline or diesel engines, natural gas engines emit lower levels of pollutants, including polycyclic aromatic hydrocarbons (PAHs), sulfur dioxide (SO<sub>2</sub>), and CO. However, owing to higher combustion temperatures in the cylinder, their NO<sub>x</sub> emissions are higher [1–3]. Additionally, various factors, such as valve overlap angle, cylinder clearance, and incomplete combustion, result in massive CH<sub>4</sub> emissions from natural gas engines [4–8]. CH<sub>4</sub> is the most challenging element to oxidize in hydrocarbon emissions, with a higher catalytic ignition temperature than other alkanes and unsaturated hydrocarbons, causing difficulty while treating emissions [9,10]. Natural gas engines with an equivalent combustion mode commonly incorporate a three-way catalytic converter as the post-treatment system to synergistically and efficiently reduce HC, CO, and other pollutants. However, the comparable combustion mode results in elevated combustion temperatures and increased NO<sub>x</sub> emissions.

Usually, an exhaust gas recirculation (EGR) system is utilized to enhance the engine's thermal burden and NO<sub>x</sub> emissions. The implementation of an EGR system is an effective solution for addressing the issues of increased thermal burden, knocking tendency, and NO<sub>x</sub> emissions in natural gas engines under equivalent combustion modes [11,12]. EGR systems with high pressure are typically favored in heavy-duty engines owing to their

durable compressors and intercoolers, responsive functionality, and mature technological level. The pressure drop in high-pressure EGR systems is determined by the difference in pressure between the vortex front pressure at the exhaust end and the intake manifold pressure at the intake end. The value of the pressure difference affects the introduction capacity of EGR. Consequently, high-pressure EGR can normally only be introduced within a specific operating range. Moreover, the intake point is located in front of the turbine; this reduces the turbine's efficiency to a certain extent. If the EGR valve is fully open and the ideal EGR rate cannot be achieved, alternative methods are required to improve and optimize the introduction ability of EGR; common methods include using Venturi tubes, adjusting throttle valves, utilizing exhaust back-pressure valves, and implementing variable nozzle turbochargers (VNTs). The application of VNT can effectively decrease nitrogen oxide emissions while maintaining the engine's power performance. It achieves this by simultaneously increasing the engine's intake and EGR rates. Furthermore, VNT increases the pressure in the pre-vortex stage post-boosting, thereby reducing the amplitude in the difference between exhaust and intake pressure. This reduction, in turn, results in smaller fluctuations in the pump air loss over time. Li et al. [13] compared the effects of different EGR rates on combustion and emissions in a spark ignition natural gas engine. The results showed that as the EGR rate increased, NO<sub>x</sub> emissions significantly decreased, and the maximum reduction in the engine's effective expansion ratio was approximately 3.88%. At high speeds, EGR had a more significant impact on the engine performance. It should be noted that cooling the circulating exhaust gas of EGR can further improve the engine performance and reduce NO<sub>x</sub> emissions. Zheng et al. [14] compared the inhibitory effects of non-cooled and cooled EGR on NO<sub>x</sub> emissions at different oxygen levels. As the intake oxygen content decreased, NO<sub>x</sub> emissions decreased. Using cooled EGR could more effectively suppress NO<sub>x</sub> emissions; hence, the exhaust gas temperature should be reduced below 120 °C for best results. Li et al. [15] conducted a study on spark ignition natural gas engines, and the results showed that regardless of the type of dilution gas, NO<sub>x</sub> emissions significantly decreased upon increasing the dilution ratio. Reynolds et al. [16] compared the effects of EGR and lean burn modes on the combustion and emission characteristics of a naturally aspirated ignition engine with a compression ratio of 10.5. The results showed that the implementation of the lean burn mode significantly improved the thermal efficiency, while EGR was more effective in reducing NO<sub>x</sub> emissions, but it also increased THC emissions more. Wijetugne et al. [17] established a VNT system based on PID control based on a numerical model of diesel engines. They used an EGR valve to control the intake flow rate, thus achieving faster transient torque control response, more precise control, and better control of exhaust smoke. Yu et al. [18] investigated the coupling effects of EGR and pilot diesel quantity on a high-pressure direct injection (HPDI) engine. The simulation indicated that NO<sub>x</sub> and soot emissions could be well-balanced at moderate EGR rates.

Engine combustion typically involves complex physical and chemical processes. The mathematical model of engine combustion is a dynamic, multivariate, and highly nonlinear system. To optimize VNT and EGR on natural gas engines, it is essential to establish the correlation between input parameters, such as VNT opening, EGR opening, ignition angle, and intake manifold pressure, and the resultant variables of torque, gas consumption rate, exhaust temperature, emissions, EGR rate, and cylinder knock indicator parameters, among others. This correlation must be based on empirical data to enable the prediction of dependence of output variables on independent input variables. Vapnik introduced the support vector machine (SVM) learning approach in 1995 [19]. SVMs aim to discover the optimal balance between model complexity and learning capacity with limited sample information. SVMs have demonstrated numerous advantages in addressing practical issues, such as small samples, nonlinearity, and high dimensionality, while also mitigating problems of 'curse of dimensionality', 'over learning', and 'under learning'. Their mathematical model is straightforward, with a solid theoretical foundation, which makes it a popular tool for regression prediction analysis, function estimation, signal processing, etc. [20–29].

EGR can effectively address the emission issue of natural gas engines with equivalent combustion. However, due to the proximity of the VNT booster's inlet and outlet as well as the high-pressure EGR system's inlet and outlet within the intake and exhaust gas pathways, there is an interaction between the airflows. Changes in control parameters for engine intake flow and EGR rates can simultaneously affect the power, economy, and emission performance of natural gas engines. Therefore, further exploration is required to understand the coupling and coordination relationship. To optimize engine performance, multiple objectives must be satisfied, including power, economy, emissions, and durability. However, different optimization objectives are frequently conflicting, including economy and emissions, maximum cylinder pressure, and front turbine temperature. Therefore, a compromise is necessary. For natural gas engines utilizing the VNT+EGR technology, the objectives involve the range of VNT regulation for EGR, EGR regulation for the ignition angle, and ignition angle regulation for NO<sub>x</sub> emissions and fuel efficiency. Multi-objective optimization aims to establish the relationships between different parameters, enabling the engine to maintain an optimal balance between power, efficiency, and emissions based on requirements. Using a VNT in this study, engine bench tests were performed to examine the effects of coordinated VNT and EGR control on the performance and emissions of identical combustion natural gas engines under varying operational conditions. Multi-objective optimization was conducted on multiple selected test operating points via SVMs that combine SVR and NSGA-II algorithms.

## 2. Materials and Methods

The experiment employed a 12.4 L, inline six-cylinder, four-stroke heavy-duty natural gas engine with spark ignition. Table 1 summarizes the engine's main technical specifications. The continuous flow (CFV) fuel supply system met the requirement for accurate fuel metering, thus enabling improved combustion, fuel efficiency, and transient response. The engine utilized an adaptive closed-loop control system equipped with a wide-range oxygen sensor to control the excess air coefficient ( $\lambda$ ). Additionally, it was equipped with a high-pressure EGR system to mitigate the high thermal burden and NO<sub>x</sub> reduction requirements resulting from equivalent combustion.

**Table 1.** Engine technical parameters.

| Items                                       | Parameters |
|---|------------|
| Bore/mm                                     | 126        |
| Stroke/mm                                   | 166        |
| Compression Ratio                           | 11.5       |
| Maximum Torque/N·m                          | 2100       |
| Speed at Maximum Torque/r·min <sup>-1</sup> | 1300       |
| Rated Power/kW                              | 330        |
| Speed at Rated Power/r·min <sup>-1</sup>    | 1800       |

The apparatus utilized for testing the engine on a bench is depicted in Figure 1. The experimental setup comprised the engine, electric dynamometer, electronic control calibration system, bench measurement and control system, control computer, gas supply system, cooling system, engine gaseous emission testing system, and engine cylinder pressure acquisition and analysis system. The equipment employed in the experiment encompassed control systems, measurement and analysis systems, and others. Table 2 presents details related to the equipment's type parameters, accuracy, and resolution.

Owing to the significant impact of VNT opening on the engine pressure difference, engine performance, and EGR driving ability, to explore the influence of different VNT openings on the introduction ability of high-pressure EGR, 1000, 1300, and 1600 r/min were selected as the representative low, medium, and high speeds, respectively. The engine was controlled to operate at 25%, 50%, 75%, and 100% load conditions of the aforementioned three speeds, and the opening of the VNT nozzle ring was adjusted accordingly. By

adjusting the EGR valve opening, different EGR rates were achieved; it should be noted that 1–3 EGR rates, including the maximum EGR rate, were selected, and the ignition angle was gradually advanced to the maximum brake torque (MBT) ignition angle or knocking edge, which was used as a representative operating point at this EGR rate. Owing to the presence of a certain amount of empty stroke in the nozzle ring of the turbocharger, further increase in the VNT opening after 70% had minimal effect on the working state of the turbocharger. Therefore, the adjustment range of the VNT opening in the test was selected to have a good linearity of 30–70%.

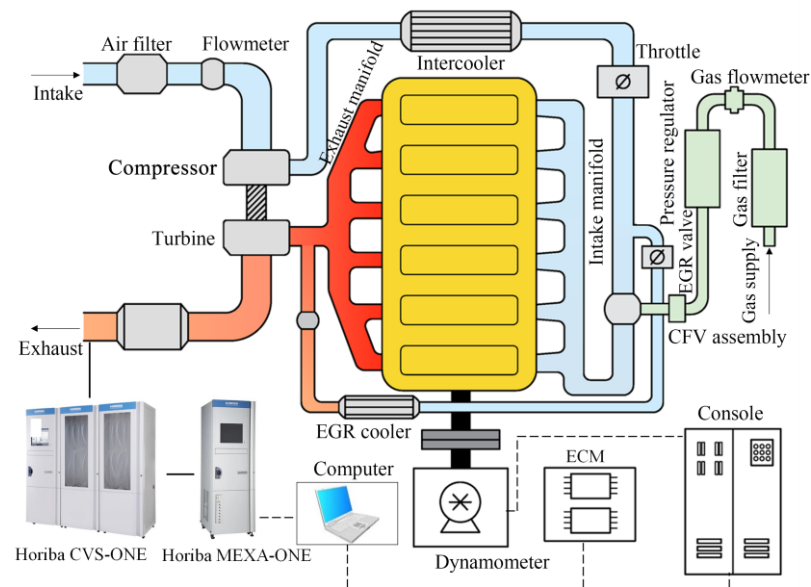


**Figure 1.** Experimental setup for engine bench testing.

**Table 2.** Main testing equipment parameters and accuracy.

| Device or System         | Type                    | Accuracy/Resolution          |
|--------------------------|-------------------------|------------------------------|
| Dynamometer              | INDY S66-4/4400-1BS-1   | $\pm 0.2\%$ N·m; $\pm 2$ r/m |
| Gas flow meter           | Toceil CMF025           | $\pm 2.5\%$                  |
| Combustion Analyzer      | Kistler Ki-box 2893B    | /                            |
| Cylinder pressure sensor | Kistler 6052Cu20        | $\pm 0.5\%$                  |
| Goniometer               | Kistler CA adapter 2619 | 0.1 CA                       |
| Signal amplifier         | Kistler 5064C           | $\pm 0.1V$                   |

To improve the generalization ability of the model, data were randomly selected from the sample data to generate training and testing sets. Among the 241 sample point data obtained in the experiment, 181 were randomly selected as the training set, and the remaining 60 were used as the testing set to evaluate the model's performance. To improve the prediction accuracy of the model, it is necessary to preprocess the data used for training the support vector regression machine model before establishing it. Owing to differences in the magnitudes of various engine parameters during the experiment, normalization is required in the preprocessing stage. Normalization can limit the input and output data within a certain range, thereby eliminating the adverse effects of singular sample data. Moreover, logarithmic transformation before normalizing the output data during support vector regression model training can further reduce the range of parameter changes, improve model fitting accuracy, and reduce model training time [30]. Therefore, in this study, base 10 logarithmic transformation was performed on the output training data, and the input and output data were normalized within the range of  $[-1, +1]$ . These normalized input and output data were used to train the support vector regression machine. The RBF kernel function can reflect the distance between two data vectors; additionally, it

exhibits a strong generalization ability and has been widely used in nonlinear models [31]. Therefore, this function was adopted in this study. When using the RBF kernel function, it is necessary to adjust its two key parameters, i.e., the penalty parameter (C) and variance (g). To achieve optimal performance, this study aimed to minimize the mean square error of the regression model and used the grid search function of libsvm to determine the optimal C and g for each regression model.

After optimizing the kernel function and regression model parameters, the model parameters were determined, and the predictive models for performance parameters at each operating point were trained. To ensure the fitting and prediction accuracy of the SVR model, it is necessary to evaluate the model. The performance of regression models is mainly reflected by the size of various errors between the fitted data and the truth. Common evaluation indicators include goodness of fit ( $R^2$ ), mean square error (MSE), and mean absolute percentage error (MAPE). The calculation formulas for each evaluation indicator are given in Equations (1)–(3).

$$R^2 = \frac{S_{SR}}{S_{ST}} = 1 - \frac{\sum_{i=1}^l (y_i^* - y_i)^2}{\sum_{i=1}^l (y_i - \bar{y})^2} \quad (1)$$

$$MSE = \frac{1}{l} \sum_{i=1}^l (y_i^* - y_i)^2 \quad (2)$$

$$MAPE = \frac{1}{l} \sum_{i=1}^l \left| \frac{y_i^* - y_i}{y_i} \right| \times 100\% \quad (3)$$

where  $S_{SR}$  is the sum of regression squares,  $S_{ST}$  is the total sum of squares,  $y_i^*$  is the predicted value of the  $i$ -th sample,  $y_i$  is the true value of the  $i$ -th sample,  $\bar{y}$  is the mean of the sample, and  $l$  is the number of samples.

The main pollutants emitted by natural gas engines are NO<sub>x</sub> and CH<sub>4</sub>; there exists a trade-off between these two main emissions as well as emissions and engine economy. According to the transient emission test of post-treated equivalent combustion natural gas engines, to meet the latest emission regulations, residual NO<sub>x</sub> emissions in each pollutant must be significantly smaller than CH<sub>4</sub> emissions. Therefore, during optimization, the main consideration should be the reduction of NO<sub>x</sub> emissions. Therefore, the final optimization problem is constructed as follows:

$$\begin{aligned} & \min \begin{cases} f_{b_e}(O_{VNT}, O_{EGR}, \theta_{ST}, P_{MAP}, n) \\ f_{NO_x}(O_{VNT}, O_{EGR}, \theta_{ST}, P_{MAP}, n) \end{cases} \\ & s.t. \begin{cases} \frac{|f_T(O_{VNT}, O_{EGR}, \theta_{ST}, P_{MAP}, n) - T_{target}|}{T_{target}} \leq 0.03 \\ f_{T_{exh}}(O_{VNT}, O_{EGR}, \theta_{ST}, P_{MAP}, n) \leq 760 \\ f_{K_{peak}}(O_{VNT}, O_{EGR}, \theta_{ST}, P_{MAP}, n) \leq 1.5 \\ f_{R_{EGR}}(O_{VNT}, O_{EGR}, \theta_{ST}, P_{MAP}, n) \leq R_{EGRmax} \\ 40 \leq O_{VNT} \leq 70 \\ 0 \leq O_{EGR} \leq 100 \\ 10 \leq \theta_{ST} \leq 50 \\ P_{MAP} \leq P_{MAPmax} \end{cases} \end{aligned} \quad (4)$$

where  $b_e$  is the effective gas consumption rate (g/kW·h),  $O_{VNT}$  is the VNT valve opening (%),  $O_{EGR}$  is the EGR valve opening (%),  $\theta_{ST}$  is the ignition advance angle (°CA BTDC),  $P_{MAP}$  is the manifold pressure (MPa),  $n$  is the engine speed,  $T$  is the brake torque (N·m),  $T_{EXH}$  is the exhaust temperature before vortex (°C),  $K_{PEAK}$  is the statistical knocking amplitude, and  $R_{EGR}$  is the EGR rate (%).

Because the constructed natural gas engine support vector regression model is a non-parametric prediction model, traditional optimization methods cannot effectively handle such problems. Compared with traditional optimization algorithms, evolutionary algorithms draw on the evolutionary operations of organisms in nature and are not limited

by the continuity and nonlinearity of optimization functions; moreover, they demonstrate high robustness and wide applicability. In evolutionary algorithms, genetic algorithms are the most mature and widely used in multi-objective optimization solutions. Among them, non-dominated sorting genetic algorithms are multi-objective genetic algorithms based on Pareto optimal solutions. However, the first generation of non-dominated sorting genetic algorithms required fitness allocation; consequently, the optimization results were somewhat influenced by the subjective thoughts of designers, and the algorithm itself had certain limitations [32]. Deb et al. [33] proposed the second-generation NSGA algorithm based on the first-generation NSGA algorithm in 2002, which is the elitist non-dominated sorting genetic algorithm (NSGA-II). Compared to the NSGA algorithm, the NSGA-II algorithm has been optimized in the following aspects: introduction of an elite retention strategy, adoption of a fast, non-dominated sorting algorithm, and introduction of a congestion comparison operator. In this study, the support vector regression model and NSGA-II algorithm were combined to solve the aforementioned problem.

### 3. Results and Discussion

#### 3.1. Impact of VNT on EGR Introduction Ability

According to the working principle of VNTs, decreasing the VNT opening reduces the cross-sectional area of the airflow, thereby enhancing the turbocharging capability of the engine and increasing the turbine speed and power output. It should be noted that excessively reducing the VNT opening in conditions with ample engine turbocharging capacity can result in engine overcharging, excess intake, and more torque than required for operation. If the VNT opening is too high, the turbocharger's boosting capacity will be insufficient, causing the engine to intake a volume that falls short of demand.

Figure 2 illustrates the effect of VNT opening on pressure drop before and after EGR and the maximum EGR rate of an equivalent combustion natural gas engine under different load conditions at a speed of 1000 r/min. At low speeds, the engine cannot introduce EGR at medium to high load conditions owing to the inability to establish a pressure drop. After using a VNT, in working conditions where the EGR could not be driven previously, as the VNT opening decreased, the engine pressure drop gradually changed from negative to positive; in other words, the exhaust pressure in front of the engine turbine gradually exceeded the intake manifold pressure. Therefore, as the VNT opening decreased, the maximum EGR rate achievable under each operating condition also significantly increased. By adjusting the VNT opening, maximum EGR rates of 17.7% and 18.4% were achieved under the 1000 r/min external characteristics and 75% load conditions; EGR could not be introduced previously under this condition. For low load conditions, owing to the large pressure drop in the engine, it was relatively easy to achieve a higher EGR rate. According to the previous analysis, after the equivalent combustion natural gas engine EGR rate exceeded 20%, the negative impact on engine combustion, power, and economy became more obvious. Therefore, during testing, when the EGR rate reached approximately 20%, it did not continue to increase. Therefore, reducing the VNT opening under low load conditions had no effect on the maximum EGR rate; it only increased the engine pressure drop. It should be noted that excessive pressure drop leads to significant pump air loss, which negatively impacts the engine economy.

Figures 3 and 4 show the effects of VNT opening on engine pressure drop and the maximum EGR rate under different load conditions of 1300 and 1600 r/min for equivalent combustion natural gas engines, respectively. The VNT adjustment range was reduced at medium to high speeds in comparison to low speeds. At a medium to high load condition of 1300 r/min, excessive VNT opening caused insufficient introduction of EGR; it is noteworthy that higher thermal burden results in excessive exhaust temperature. However, when the VNT opening was too small, it increased the pressure under medium to high loads. Under the condition of the EGR rate not exceeding 20%, a significantly small VNT opening can cause the torque to exceed the operating requirements. Therefore, the optimal adjustment range of VNT under external characteristics of 1300 r/min was 47–53% and 50–60% under

75% and 50% load conditions, respectively. Compared to 1300 r/min, a higher speed resulted in more intake flow; hence, the turbocharger achieved a maximum EGR rate of 20% at 55% opening. A higher EGR rate could also be achieved at larger VNT openings.

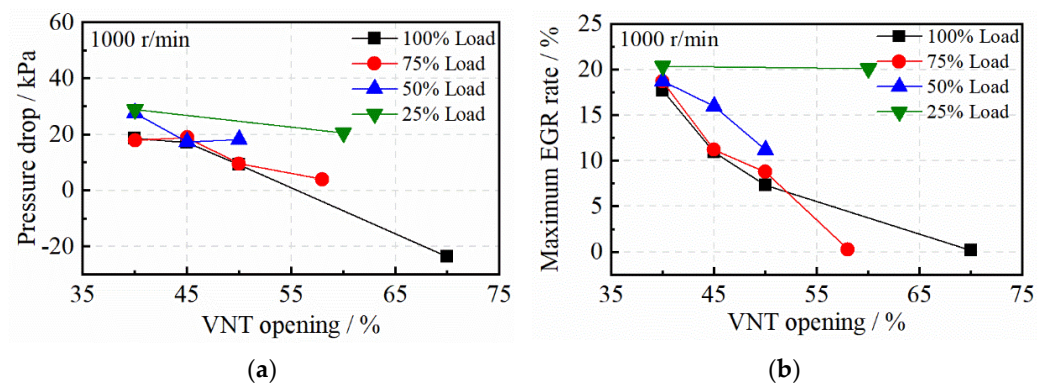


**Figure 2.** Influence of VNT opening on pressure drop and maximum EGR rate under 1000 r/min. (a) EGR pressure drop. (b) Maximum EGR rate.

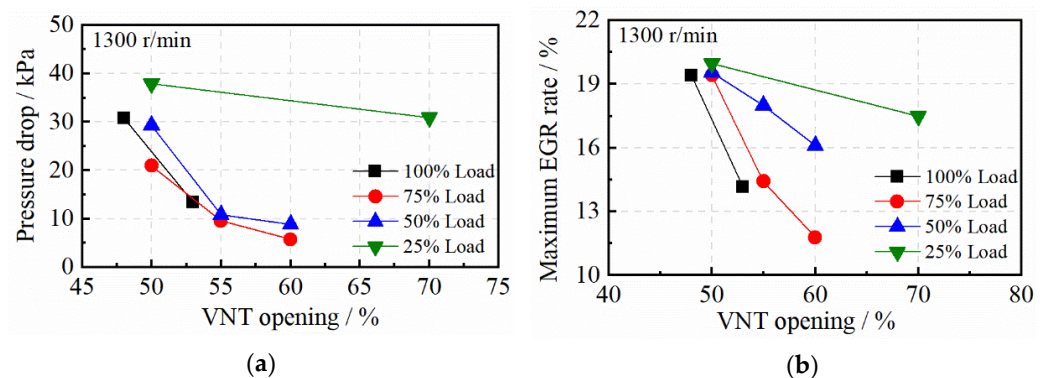


**Figure 3.** Influence of VNT opening on pressure drop and maximum EGR rate under 1300 r/min. (a) EGR pressure drop. (b) Maximum EGR rate.

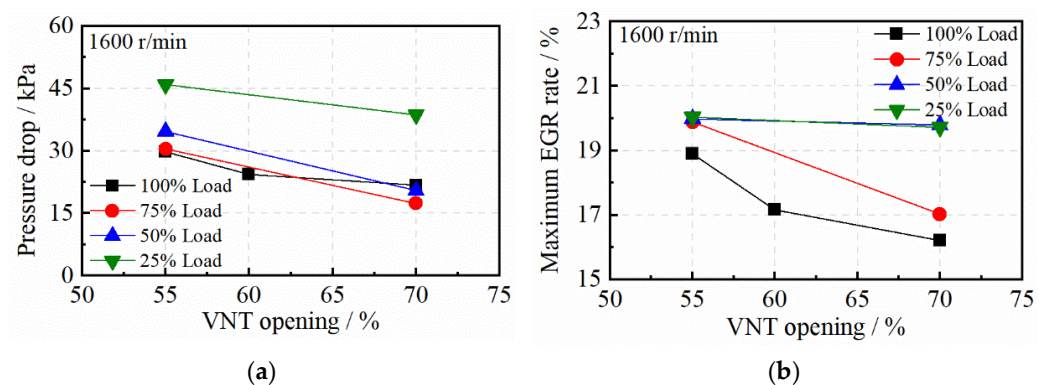


**Figure 4.** Influence of VNT opening on pressure drop and maximum EGR rate under 1600 r/min. (a) EGR pressure drop. (b) Maximum EGR rate.

### 3.2. Impact of VNT-Coupled EGR on Engine Economy and Emissions

Figure 5 shows the effects of VNT and EGR on the fuel efficiency of equivalent combustion natural gas engines under different operating conditions at a speed of 1000 r/min. The black, red, and blue data points in the figure represent external characteristic operating conditions, 75% load operating conditions, and 50% load operating conditions, respectively. Different data point shapes represent different VNT openings, and the opening values are indicated next to the data points. Owing to the sufficient introduction capacity of the

engine, the performance difference in the engine after adopting VNT was not significant under the 25% load condition; to avoid interference, it is not included in the comparison chart. By adjusting the VNT opening, the engine could operate at different EGR rates. As the VNT opening gradually decreased, the range of EGR rate adjustment gradually increased. The increase in the upper limit of the EGR rate can mainly be attributed to the decrease in VNT opening, which increased the engine pressure drop and enhanced the driving ability of EGR. Meanwhile, the increase in the lower limit of the EGR rate was mainly caused by the increase in engine turbocharging capacity. When the EGR rate is too low, it leads to excessive intake pressure and changes in engine operating conditions. Comparing the data under the same load conditions, as the VNT opening decreased, the minimum gas consumption rate gradually decreased. For example, under external characteristic conditions, a minimum gas consumption of 187.5 g/W·h was observed at 40% VNT opening and 17.6% EGR rate.

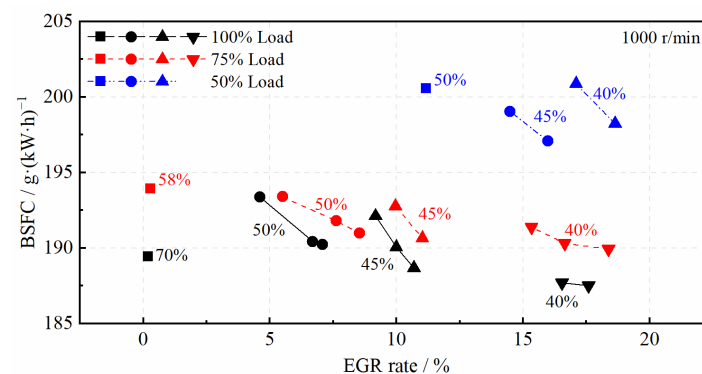


Figure 5. Influence of VNT-coupled EGR on BSFC under 1000 r/min.

Figure 6 shows the effects of VNT and EGR on the fuel efficiency of equivalent combustion natural gas engines under different operating conditions (medium speed, 1300 r/min; high speed, 1600 r/min). Owing to the high thermal burden of the engine at medium and high speeds, a smaller EGR rate could not be used; thus, the range of VNT opening adjustment was reduced, and the effect of EGR boundary expansion due to VNT was weakened. At this speed, although reducing the VNT opening could still improve the adjustment range of the EGR rate, it did not optimize the gas consumption rate. The optimal value of gas consumption was observed at a moderate VNT opening. In the high-speed range, the control range of the EGR rate was narrower, and the impact of adjusting the VNT was smaller. However, under some loads, the EGR rate increased, and air consumption increased in comparison to the raw engine.

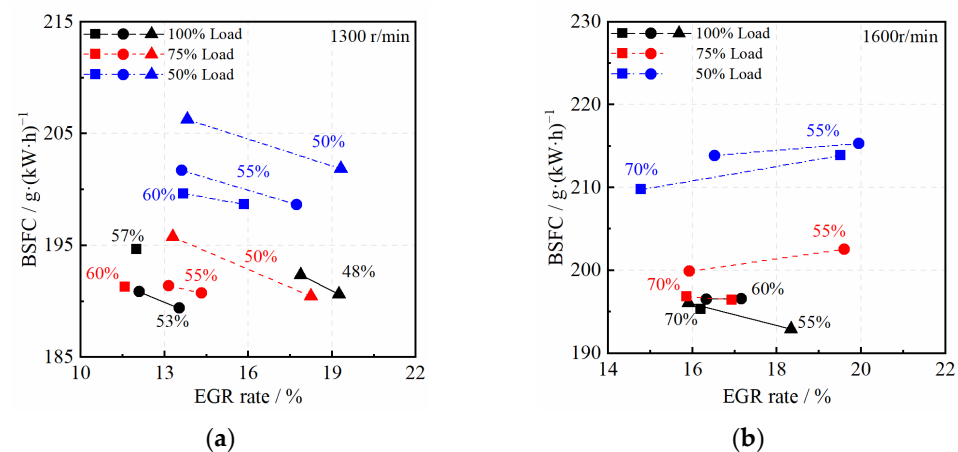


Figure 6. Influence of VNT-coupled EGR on BSFC under 1300 and 1600 r/min. (a) 1300 r/min. (b) 1600 r/min.

Figure 7 shows the effects of VNT and EGR on NO<sub>x</sub> emissions from equivalent combustion natural gas engines under different operating conditions at a speed of 1000 r/min. For equivalent combustion natural gas engines, NO<sub>x</sub> emissions are mainly dominated by the high combustion temperature in the cylinder, and a larger EGR rate can significantly reduce the combustion temperature in the cylinder, thus significantly reducing NO<sub>x</sub> emissions. NO<sub>x</sub> emissions exhibited a nearly linear variation with EGR. The influence of VNT opening on NO<sub>x</sub> emissions was relatively small, and the main effect involved changes in the EGR regulation range of the engine. In operating conditions where the raw engine had no or poor EGR introduction capacity, a higher proportion of EGR introduction could be achieved by changing the VNT opening, which significantly reduced NO<sub>x</sub>. After the introduction of EGR, high NO<sub>x</sub> emissions of the raw engine at 1000 r/min and 75% load conditions were reduced from 13.09 and 14.04 g/W·h to approximately 4.33 and 3.76 g/W·h, exhibiting a decrease of approximately 66.9% and 73.2%, respectively.

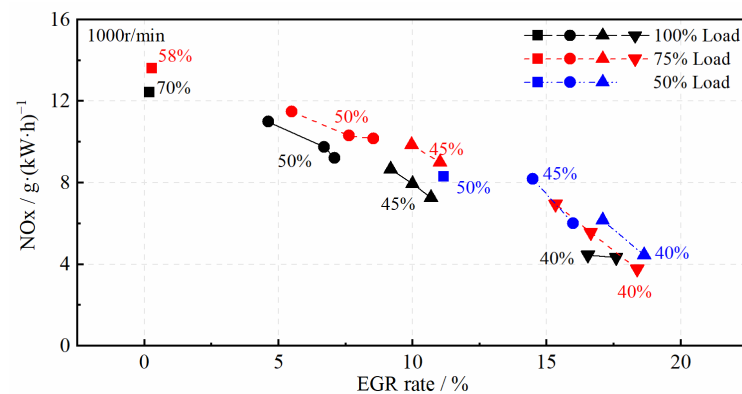
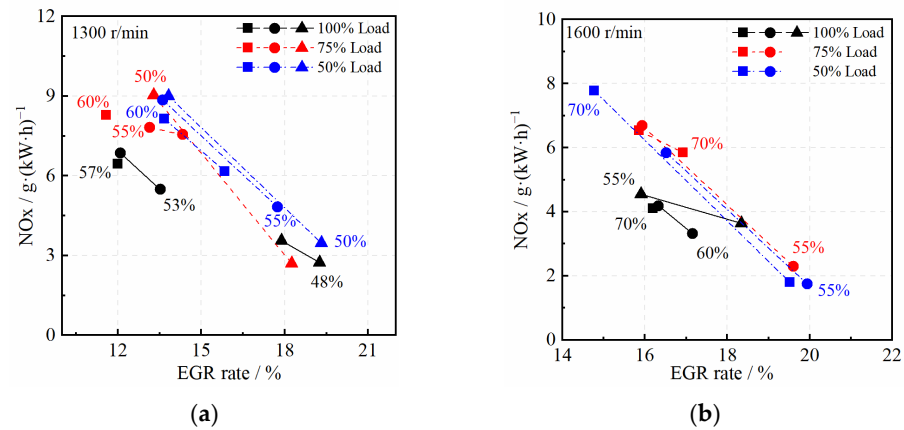


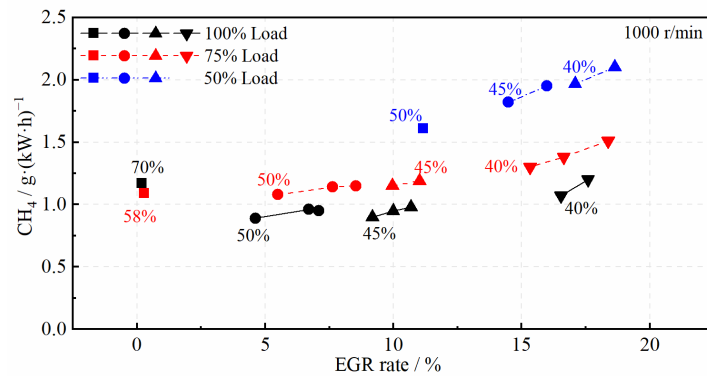
Figure 7. Influence of VNT-coupled EGR on NO<sub>x</sub> emissions under 1000 r/min.

Figure 8 shows the effects of the VNT and EGR on NO<sub>x</sub> emissions from equivalent combustion natural gas engines under different operating conditions at medium and high speeds of 1300 and 1600 r/min, respectively. Similarly to 1000 r/min, under the same operating conditions, NO<sub>x</sub> emissions were mainly affected by changes in the EGR rate and less affected by the VNT opening. By comparing the curves of different VNT openings under the same operating condition, it was evident that a decrease in the VNT opening could increase the upper limit of EGR rate regulation, thereby further reducing NO<sub>x</sub> emissions. However, at the same EGR rate, a decrease in the VNT opening slightly increased NO<sub>x</sub> emissions. Therefore, similarly to the results of the gas consumption rate, obtaining the ideal EGR rate at a moderate VNT opening could lead to optimal NO<sub>x</sub> emissions. Compared with the 1000 r/min operating condition, as the speed increased, the raw engine could achieve a certain EGR rate; thus, the optimization amplitude of VNT and EGR on NO<sub>x</sub> emissions decreased. For the 75% load condition at 1300 and 1600 r/min with high NO<sub>x</sub> emissions from the raw engine, NO<sub>x</sub> emissions could be reduced from 7.85 and 5.54 g/W·h to a maximum of 2.69 and 3.31 g/W·h, exhibiting a reduction of approximately 65.7% and 40.3%, respectively.

Figure 9 shows the effects of VNT and EGR on CH<sub>4</sub> emissions from equivalent combustion natural gas engines under different operating conditions at a speed of 1000 r/min. CH<sub>4</sub> emissions are the second largest emissions produced by natural gas engines, and their emission trends are the opposite of those of NO<sub>x</sub>. The regularity of CH<sub>4</sub> emissions was more evident, exhibiting a nearly linear increase with the EGR rate. According to engine emission testing, the CH<sub>4</sub> emission margin of the equivalent combustion natural gas engine combined with high-efficiency TWC was relatively large; therefore, it was more inclined to reduce NO<sub>x</sub> emissions when optimizing emissions. Compared with the decrease in NO<sub>x</sub>, the comprehensive effect of increasing the EGR rate on CH<sub>4</sub> was not significant. For example, under external characteristic conditions, CH<sub>4</sub> emissions increased from 1.11 to 1.20 g/W·h, exhibiting an increase of approximately 8.1%. Under 75% load characteristic conditions, CH<sub>4</sub> emissions increased from 1.20 to 1.51 g/W·h, exhibiting an increase of approximately 25.8%.



**Figure 8.** Influence of VNT-coupled EGR on NOx emissions under 1300 and 1600 r/min. (a) 1300 r/min. (b) 1600 r/min.



**Figure 9.** Influence of VNT-coupled EGR on methane emissions under 1000 r/min.

Figure 10 shows the effects of VNT and EGR on CH4 emissions from equivalent natural gas engines under different operating conditions at medium and high speeds of 1300 and 1600 r/min, respectively. Under the same operating conditions, CH4 emissions were almost not affected by changes in the VNT opening; they only changed with changes in the EGR rate. At high EGR rates with good economic efficiency and NOx emissions, CH4 emissions from the raw engine increased from 2.25 and 2.79 g/W·h to 2.43 and 3.17 g/W·h at 50% load conditions at 1300 and 1600 r/min, exhibiting an increase of approximately 8.0% and 13.7%, respectively.

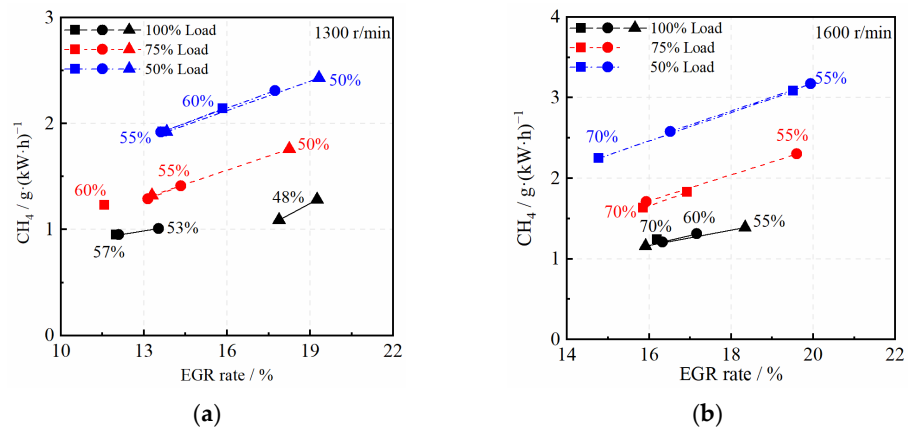


**Figure 10.** Influence of VNT-coupled EGR on methane emissions under 1300 and 1600 r/min. (a) 1300 r/min. (b) 1600 r/min.

### 3.3. Validation and Analysis of Multi-Objective Optimization Results

The training and testing sets used to establish the model were evaluated; the results are summarized in Table 3. Except  $K_{peak}$ , the determination coefficients in all output parameters were above 0.97, and the MSE was relatively small in the order of magnitude of each parameter, with an average relative error of less than 5%. The evaluation parameter data were good, indicating that the established model had good accuracy and generalization ability to meet the demand for predicting the output parameters of natural gas engines based on input parameters. The error of  $K_{peak}$  in the parameters was relatively large, mainly due to the weak correlation between the cylinder detonation situation and input parameters, thus slightly decreasing the prediction accuracy. However, the MAPE was still within 10%; the value of this parameter itself was small, and the actual difference due to a slight increase in relative deviation was not significant. Therefore, good predictions could still be made for the cylinder knocking situation.

**Table 3.** Evaluation of output parameters of support vector regression model.

| Sample       | Parameter      | Torque (N·m) | BSFC (g/kW·h) | Temperature (°C) | NOx (g/kW·h) | CH <sub>4</sub> (g/kW·h) | EGR Rate (%) | $K_{peak}$ (-) |
|--------------|----------------|--------------|---------------|------------------|--------------|--------------------------|--------------|----------------|
| Training set | R <sup>2</sup> | 0.998        | 0.991         | 0.997            | 0.980        | 0.997                    | 0.999        | 0.933          |
|              | MSE            | 164.1        | 0.53          | 2.09             | 0.066        | 0.001                    | 0.006        | 0.008          |
|              | MAPE (%)       | 0.43         | 0.08          | 0.11             | 1.85         | 0.50                     | 0.24         | 4.86           |
| Testing set  | R <sup>2</sup> | 0.995        | 0.965         | 0.993            | 0.955        | 0.991                    | 0.975        | 0.909          |
|              | MSE            | 1211.1       | 3.91          | 18.87            | 0.385        | 0.005                    | 0.493        | 0.025          |
|              | MAPE (%)       | 1.53         | 0.56          | 0.43             | 4.93         | 2.30                     | 3.67         | 9.68           |

The programming implementation was based on Python3 (libSVM and geatpy). When running a genetic algorithm, it is necessary to set the algorithm parameters. Because there is currently no theoretical guidance for various application fields, the algorithm parameters are usually set based on specific problems. The population size refers to the number of individuals in a population. According to previous research results, a population that is too large cannot optimize the algorithm results. Therefore, it is necessary to select a moderate population size, which was set to 50 in this study. The probability of crossing should generally be relatively high, with an optimal value between 0.8 and 0.95. In this study, it was set to 0.8. Furthermore, the probability of variation should generally be small, ranging between 0.05 and 0.1. In this study, it was set to 0.05. It should be noted that it is better to have a larger number of iterations, but excessive iterations can affect the algorithm's efficiency; hence, it was set to 200. Based on the aforementioned model parameters, optimization was performed for various operating conditions within the commonly used speed range. Among the obtained optimal parameter combinations and based on some boundary conditions obtained from testing, the smoothness of the control MAP was considered. Accordingly, within a reasonable range of control parameters, the calibration variable combinations for the optimal solutions of each operating condition were obtained. On the basis of optimizing the control MAP, interpolation was used to process the operating conditions between each optimized condition. The final optimized engine VNT opening, EGR valve opening, and ignition angle control MAP are shown in Figures 11–13.

By using the ECU control software, the optimized calibration control MAP data were input into the control program and synchronized with the ECU; furthermore, experimental verification was conducted at 20 operating points. Figure 14 shows the comparison between the measured and simulated values of air consumption rate, torque, vortex front temperature, EGR rate, NOx emissions, and CH<sub>4</sub> emissions for 20 main test conditions under various operating conditions using optimized control strategies. Except NOx, the relative errors of each parameter were relatively small. In most operating conditions, the experimental and simulation values exhibited good consistency. The relative errors of

almost all operating points were within 5%. The operating points with larger relative errors were mainly concentrated in the high-speed and low-load range. Engine operation under these operating conditions was relatively unstable, and there may be some data differences in multiple measurements. This is one of the reasons for the large data deviation under these operating conditions. For NO<sub>x</sub> emissions, a significant deviation was observed between the experimental and simulated values under some operating conditions, with a relative error of less than 10% in most operating conditions. In some individual operating conditions, such as high speed or low load, it was observed to be 15–20%. This can be attributed to the large range of NO<sub>x</sub> changes between different operating conditions during testing, as well as the large range selected, which decreased the testing accuracy, and a certain measurement error when testing operating conditions with low NO<sub>x</sub> emissions. Meanwhile, the average relative error of NO<sub>x</sub> emissions during regression model training was relatively large compared to other parameters. Therefore, under the superposition of errors, the error between test and simulation values was slightly larger at individual operating points, but it was small at most operating points; moreover, the absolute error value of NO<sub>x</sub> emissions was actually not large owing to the small numerical value. Therefore, the use of support vector regression modeling and the NSGA-II genetic algorithm for multi-objective optimization of the VNT+EGR equivalent combustion natural gas engine control strategy was feasible, and the obtained optimization results were relatively reliable.

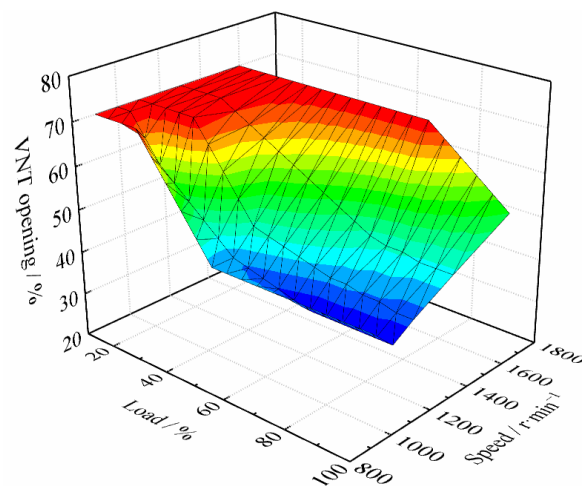


Figure 11. Optimized VNT opening calibration MAP.

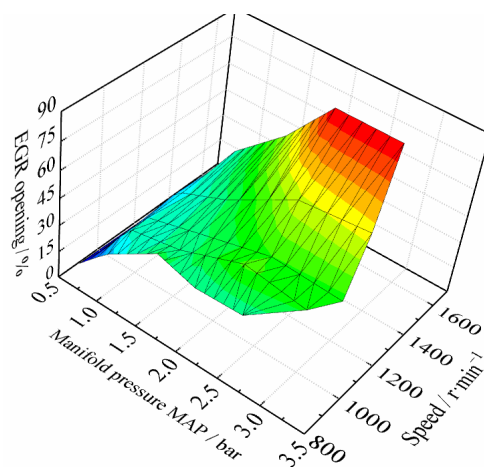


Figure 12. Optimized EGR opening calibration MAP.

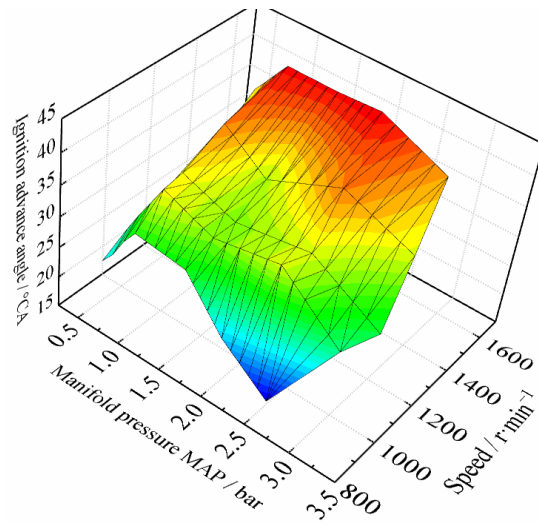


Figure 13. Optimized ignition angle opening calibration MAP.

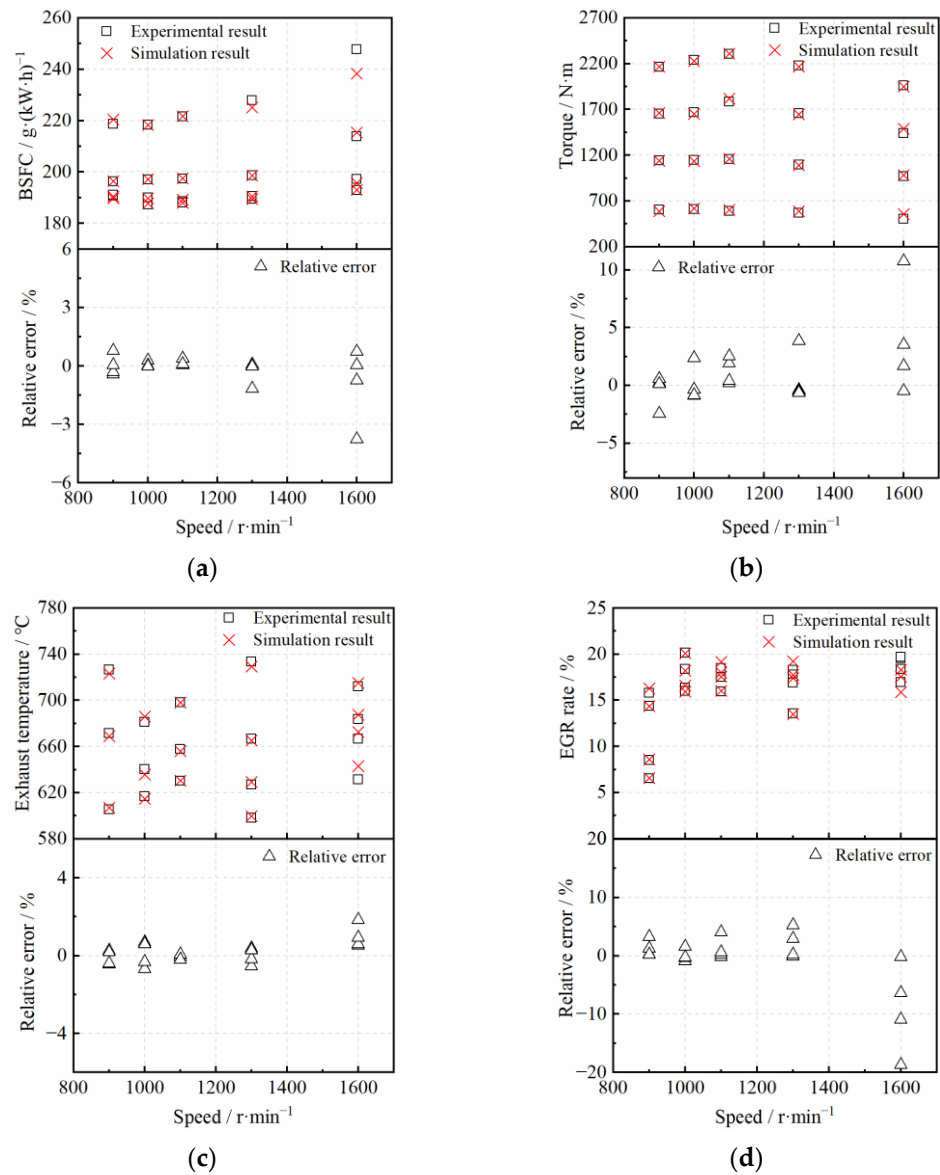
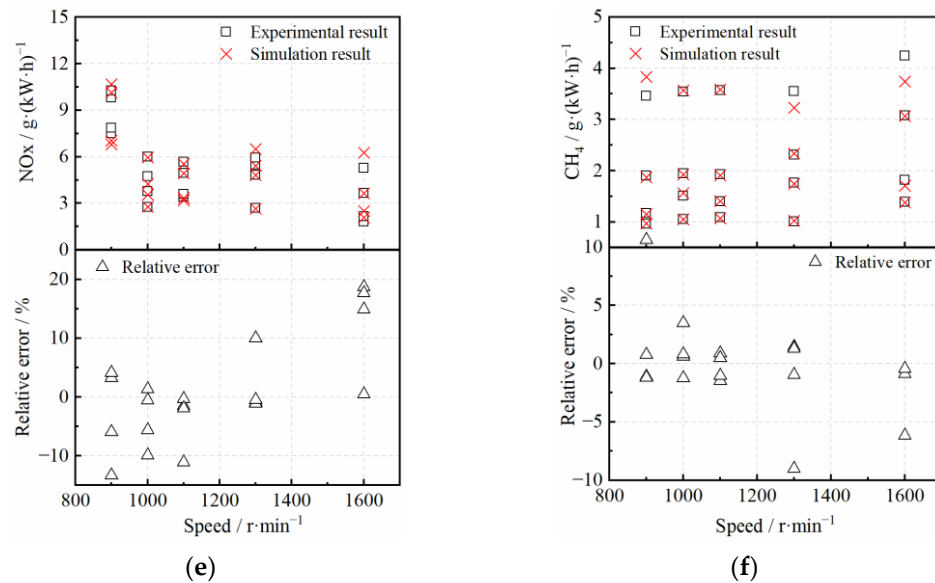


Figure 14. Cont.



**Figure 14.** Comparison between experimental and simulation values of 20 operating conditions tested after optimizing control strategies. (a) BSFC. (b) Torque. (c) Exhaust temperature. (d) EGR rate. (e) NO<sub>x</sub> emissions. (f) CH<sub>4</sub> emissions.

Under the 20 selected optimization operating conditions, changes in economic performance and emission indicators before and after the optimization of the engine control strategy were compared, as shown in Figures 15–17. Figure 15 shows the relative change in specific gas consumption between the optimized and original strategies, with negative values indicating a decrease in optimized gas consumption compared to the raw engine. With the optimized strategy, the engine gas consumption somewhat decreased under most operating conditions. The most significant decrease in gas consumption was observed at the 25% load position; this is because the original gas consumption in this part of the working condition was relatively high, and the original control strategy was not sufficiently optimized, resulting in a large space for the reduction of the gas consumption rate. Therefore, after optimization, the gas consumption rate significantly decreased. For the external characteristic point and 75% load point of the raw engine with better gas consumption, in the low to medium speed range of 1000 and 1100 r/min, owing to the improved EGR introduction ability brought by the VNT, the knocking problem was alleviated, the ignition angle could be controlled at a better position, combustion was optimized, and the gas consumption rate was significantly reduced; compared with the raw engine operating conditions, it achieved a reduction of more than 2.0 g/W·h. In the low speed range, such as the external characteristic working condition of 900 r/min, owing to the introduction of EGR, the torque slightly decreased compared to that of the raw engine, thus slightly increasing the fuel consumption rate. After the engine speed increased, the VNT opening remained relatively large, with little difference from the original turbocharger's boosting effect. Therefore, the engine's economic performance did not significantly change, and it even showed an upward trend at some operating points. Furthermore, changes in the gas consumption rate under each test condition were compared to those under the corresponding conditions of the raw engine; the results showed that the average BSFC reduction for the 20 test conditions was 0.94%.

Figure 16 shows the changes in NO<sub>x</sub> emissions in comparison to those in the original strategy using the optimized control strategy. The optimized strategy reduced NO<sub>x</sub> emissions under all test conditions for equivalent combustion natural gas engines. From the optimization range of NO<sub>x</sub> emissions, the high load range at medium and low speeds was the most significant, with a maximum reduction at 75% load and 1000 r/min, which could be reduced from the raw engine's 14.0 to 3.8 g/W·h. This is mainly because the raw engine could not introduce EGR under these operating conditions. After replacing the VNT and

optimizing the control strategy, better combustion effects were achieved. Similarly to the optimization of the gas consumption rate, the optimization effect was better at medium and low speeds, while at medium and high speeds, the optimization effect on NOx emissions of equivalent combustion natural gas engines through VNT and optimization strategies was average. On average, NOx reduction under the 20 test conditions was approximately 47.0%.

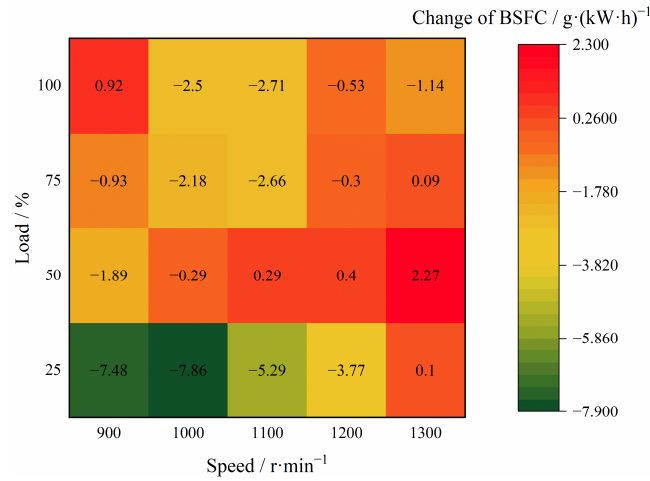


Figure 15. Optimization of BSFC for 20 selected main operating conditions.

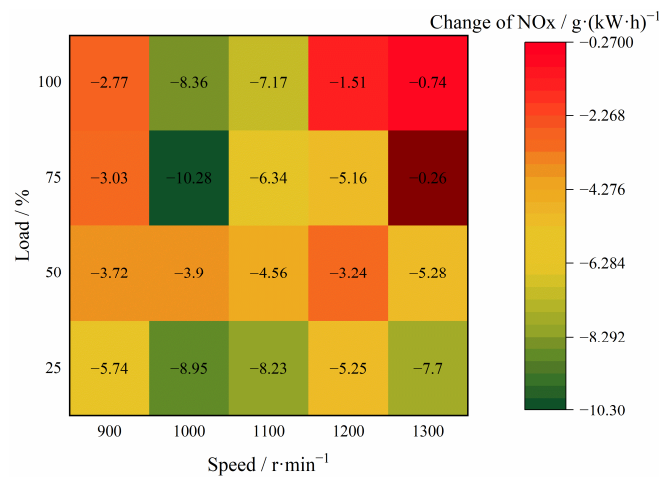


Figure 16. Optimization of NOx emission for 20 selected main operating conditions.

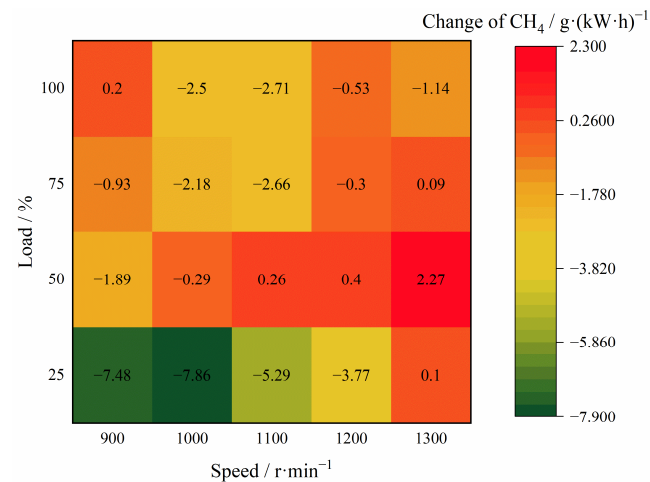


Figure 17. Optimization of methane emissions for 20 selected main operating conditions.

Figure 17 shows the changes in CH<sub>4</sub> emissions compared to those in the original control strategy using the optimized control strategy. Owing to the focus of control strategy optimization on NO<sub>x</sub> emissions from natural gas engines, CH<sub>4</sub> emissions increased under most operating conditions. Moreover, under operating conditions where NO<sub>x</sub> reduction was more significant, the increase in CH<sub>4</sub> emissions was more significant. However, the overall change in CH<sub>4</sub> emissions was much smaller than the optimization effect on NO<sub>x</sub> emissions, with an average increase of only 3.7% in CH<sub>4</sub> emissions under 20 operating conditions.

#### 4. Conclusions

To solve the contradiction between the economy and emissions of natural gas engines, the impact of a VNT-coupled EGR system on the economy and emissions of natural gas engines was analyzed. Accordingly, a support vector regression machine model for natural gas engines was established and combined with a genetic algorithm. Subsequently, multi-objective optimization was performed on the control strategy of VNT-coupled EGR for natural gas engines; thus, the economy and emissions could be comprehensively optimized. The conclusions derived from this study are discussed below:

1. The use of VNTs in equivalent combustion natural gas engines can enhance the ability to introduce EGR under multiple operating conditions and expand the range of EGR regulation, thereby reducing the engine thermal load, improving fuel efficiency, and reducing emissions. As the VNT opening decreased, the maximum EGR rate achievable under various operating conditions also significantly increased. By adjusting the VNT opening, maximum EGR rates of 17.7% and 18.4% could be achieved under the 1000 r/min external characteristic and 75% load conditions, respectively; it should be noted that previously, under these conditions, EGR could not be introduced.
2. Under medium to high speed operating conditions, owing to the higher engine thermal burden, the range of VNT opening adjustment became narrower. Although reducing the VNT opening could still improve the maximum EGR rate, it did not optimize the economic performance. Thus, adopting a medium VNT opening resulted in better thermal efficiency. Compared to 1300 r/min, a higher speed brought more intake flow; hence, the turbocharger could achieve a maximum EGR rate of 20% at 55% opening.
3. The regularity of CH<sub>4</sub> emissions was more obvious, exhibiting a nearly linear increase with the EGR rate. Under the same operating conditions, CH<sub>4</sub> emissions were almost unaffected by changes in the VNT opening and only varied with changes in the EGR rate.
4. The multi-objective optimization method based on a support vector regression model and NSGA-II genetic algorithm effectively optimized VNT and EGR control parameters, thus slightly improving the economy and significantly reducing NO<sub>x</sub> emissions, while maintaining the original engine power performance. At 20 optimized validation operating points, the average decrease in BSFC was 0.94%, the average decrease in NO<sub>x</sub> was 47.0%, and the average increase in CH<sub>4</sub> was 3.7%.

**Author Contributions:** Conceptualization, D.L. and L.F.; methodology, Y.R.; investigation, Y.R. and L.F.; writing—original draft preparation, K.Z. and Y.R.; writing—review and editing, K.Z. and Y.Z.; Visualization, K.Z.; supervision, D.L. and Y.Z.; project administration, D.L. All authors have read and agreed to the published version of the manuscript.

**Funding:** This research was funded by the National Key R&D Program of China, grant number 2022YFE0100100.

**Data Availability Statement:** The raw data supporting the conclusions of this article will be made available by the authors on request.

**Conflicts of Interest:** Author Lanlan Fan was employed by the company Jinan Power Co., Ltd., Sinotruk Group. The remaining authors declare that the research was conducted in the absence of any commercial or financial relationships that could be construed as a potential conflict of interest.

## References

1. Chen, H.; He, J.; Zhong, X. Engine combustion and emission fuelled with natural gas: A review. *J. Energy Inst.* **2018**, *92*, 1123–1136. [[CrossRef](#)]
2. Thiruvengadam, A.; Besch, M.; Carder, D.; Oshinuga, A.; Pasek, R.; Hogo, H.; Gautam, M. Unregulated greenhouse gas and ammonia emissions from current technology heavy-duty vehicles. *J. Air Waste Manag. Assoc.* **2016**, *66*, 1045–1060. [[CrossRef](#)] [[PubMed](#)]
3. Schröder, A.; Eicheldinger, S.; Prager, M.; Jaensch, M. Experimental mild conversion of a lean burn natural gas engine with SCR to a hydrogen engine: NO<sub>x</sub> and GWP potential for marine applications. *Int. J. Engine Res.* **2023**, *24*, 2369–2387. [[CrossRef](#)]
4. Xin, M.; Gan, H.; Cong, Y.; Wang, H. Numerical simulation of methane slip from marine dual-fuel engine based on hydrogen-blended natural gas strategy. *Fuel* **2024**, *358*, 130132. [[CrossRef](#)]
5. Wei, L.; Geng, P. A review on natural gas/diesel dual fuel combustion, emissions and performance. *Fuel Process. Technol.* **2016**, *142*, 264–278. [[CrossRef](#)]
6. Kim, S.; Park, C.; Jang, H.; Kim, C.; Kim, Y. Effect of boosting on a performance and emissions in a port fuel injection natural gas engine with variable intake and exhaust valve timing. *Energy Rep.* **2021**, *7*, 4941–4950. [[CrossRef](#)]
7. Shu, J.; Fu, J.; Liu, J.; Ma, Y.; Wang, S.; Deng, B.; Zeng, D. Effects of injector spray angle on combustion and emissions characteristics of a natural gas (NG)-diesel dual fuel engine based on CFD coupled with reduced chemical kinetic model. *Appl. Energy* **2019**, *233–234*, 182–195. [[CrossRef](#)]
8. Li, Y.; Li, H.; Guo, H.; Li, Y.; Yao, M. A numerical investigation on methane combustion and emissions from a natural gas-diesel dual fuel engine using CFD model. *Appl. Energy* **2017**, *205*, 153–162. [[CrossRef](#)]
9. Gong, J.; Wang, D.; Li, J.; Currier, N.; Yezerets, A. Dynamic oxygen storage modeling in a three-way catalyst for natural gas engines: A dual-site and shrinking-core diffusion approach. *Appl. Catal. B Environ.* **2017**, *203*, 936–945. [[CrossRef](#)]
10. Lehtoranta, K.; Koponen, P.; Vesala, H.; Kallinen, K.; Maunula, T. Performance and Regeneration of Methane Oxidation Catalyst for LNG Ships. *J. Mar. Sci. Eng.* **2021**, *9*, 111. [[CrossRef](#)]
11. Lu, X.; Wei, L.; Zhong, J. Effects of Injection Overlap and EGR on Performance and Emissions of Natural Gas HPDI Marine Engine. *Combust. Sci. Technol.* **2024**, *196*, 37–54. [[CrossRef](#)]
12. Wu, B.; Luo, Y.; Feng, Y.; Zhu, C.; Yang, P. Design and thermodynamic analysis of solid oxide fuel cells–internal combustion engine combined cycle system based on Two-Stage waste heat preheating and EGR. *Fuel* **2023**, *342*, 127817. [[CrossRef](#)]
13. Li, Y.; Wang, P.; Wang, S.; Liu, J.; Xie, Y.; Li, W. Quantitative investigation of the effects of CR, EGR and spark timing strategies on performance, combustion and NO<sub>x</sub> emissions characteristics of a heavy-duty natural gas engine fueled with 99% methane content. *Fuel* **2019**, *255*, 115803.115801–115803.115810. [[CrossRef](#)]
14. Zheng, M.; Irick, D.K.; Hodgson, J. Stabilizing Excessive EGR With an Oxidation Catalyst on a Modern Diesel Engine. In Proceedings of the ASME 2002 Internal Combustion Engine Division Spring Technical Conference, Rockford, IL, USA, 14–17 April 2002.
15. Li, W.; Liu, Z.; Wang, Z.; Xu, Y. Experimental investigation of the thermal and diluent effects of EGR components on combustion and NO<sub>x</sub> emissions of a turbocharged natural gas SI engine. *Energy Convers. Manag.* **2014**, *88*, 1041–1050. [[CrossRef](#)]
16. Reynolds, C.C.O.B.; Evans, R.L. Improving emissions and performance characteristics of lean burn natural gas engines through partial stratification. *Int. J. Engine Res.* **2005**, *5*, 105–114. [[CrossRef](#)]
17. Wijetunge, R.S.; Hawley, J.G.; Vaughan, N.D. An exhaust pressure control strategy for a diesel engine. *Proc. Inst. Mech. Eng. Part D J. Automob. Eng.* **2004**, *218*, 449–464. [[CrossRef](#)]
18. Yu, S.; Wei, L.; Zhou, S.; Lu, X.; Huang, W. Numerical Study on the Effects of Pilot Diesel Quantity Coupling EGR in a High Pressure Direct Injected Natural Gas Engine. *Combust. Sci. Technol.* **2024**, *196*, 1–18. [[CrossRef](#)]
19. Vapnik, V.; Vapnik, V. *The Natural of Statistical Learning Theory*; Springer: New York, NY, USA, 1995.
20. Li, Y.; Gong, S.; Sherrah, J.; Liddell, H. Support vector machine based multi-view face detection and recognition. *Image Vis. Comput.* **2004**, *22*, 413–427. [[CrossRef](#)]
21. Shih, P.; Liu, C. Face detection using discriminating feature analysis and Support Vector Machine. *Pattern Recognit.* **2004**, *39*, 260–276. [[CrossRef](#)]
22. Dong, J.X.; Krzyżak, A.; Suen, C.Y. An improved handwritten Chinese character recognition system using support vector machine. *Pattern Recognit. Lett.* **2005**, *26*, 1849–1856. [[CrossRef](#)]
23. Campbell, W.M.; Campbell, J.P.; Gleason, T.P.; Reynolds, D.A.; Shen, W. Speaker Verification Using Support Vector Machines and High-Level Features. *IEEE Trans. Audio Speech Lang. Process.* **2007**, *15*, 2085–2094. [[CrossRef](#)]
24. Peng, G.; Wang, W.S.Y. Tone recognition of continuous Cantonese speech based on support vector machines. *Speech Commun.* **2005**, *45*, 49–62. [[CrossRef](#)]
25. Melgani, F.; Bruzzone, L. Classification of hyperspectral remote sensing images with support vector machines. *IEEE Trans. Geosci. Remote Sens.* **2004**, *42*, 1778–1790. [[CrossRef](#)]
26. Chi, M.; Bruzzone, L. Semisupervised Classification of Hyperspectral Images by SVMs Optimized in the Primal. *IEEE Trans. Geosci. Remote Sens.* **2007**, *45*, 1870–1880. [[CrossRef](#)]
27. Chi, M.; Feng, R.; Bruzzone, L. Classification of hyperspectral remote-sensing data with primal SVM for small-sized training dataset problem. *Adv. Space Res.* **2008**, *41*, 1793–1799. [[CrossRef](#)]

28. Yang, Y.; Chen, R.S.; Ye, Z.B. Combination of particle-swarm optimization with least-squares support vector machine for FDTD time series forecasting. *Microw. Opt. Technol. Lett.* **2006**, *48*, 141–144. [[CrossRef](#)]
29. Osowski, S.; Hoai, L.T.; Markiewicz, T. Support vector machine-based expert system for reliable heartbeat recognition. *IEEE Trans. Biomed. Eng.* **2004**, *51*, 582–589. [[CrossRef](#)]
30. Wong, K.I.; Wong, P.K.; Cheung, C.S.; Vong, C.M. Modeling and optimization of biodiesel engine performance using advanced machine learning methods. *Energy* **2013**, *55*, 519–528. [[CrossRef](#)]
31. Keerthi, S.S.; Lin, C.J. Asymptotic Behaviors of Support Vector Machines with Gaussian Kernel. *Neural Comput.* **2003**, *15*, 1667–1689. [[CrossRef](#)] [[PubMed](#)]
32. Zitzler, E.; Thiele, L. Multiobjective evolutionary algorithms: A comparative case study and the strength Pareto approach. *IEEE Trans. Evol. Comput.* **1999**, *3*, 257–271. [[CrossRef](#)]
33. Edupuganti, V.; Prasad, M.; Ravi, V. A fast and elitist multiobjective genetic algorithm: NSGA-II. *Int. J. Comput. Inf. Syst. Ind. Manag. Appl. IJCSIM* **2010**, *2*, 121–136.

**Disclaimer/Publisher’s Note:** The statements, opinions and data contained in all publications are solely those of the individual author(s) and contributor(s) and not of MDPI and/or the editor(s). MDPI and/or the editor(s) disclaim responsibility for any injury to people or property resulting from any ideas, methods, instructions or products referred to in the content.